

TRAIL signalling promotes entosis in colorectal cancer - Supplementary File 1

2020-08-13

Contents

Abbreviations	2
Software packages	3
Figure panels for Figure 6 in the main manuscript	4
Figure 6 panel B	4
Figure 6 panel C	5
Figure 6 panel D	6
Figure 6 panel F	7
Figure 6 panel G	8
Figure 6 panel H	9
Supplementary Figures	10
Supplementary Figure 1	10
Supplementary Figure 2	11
Supplementary Figure 3	12
Supplementary Figure 4	13
Supplementary Figure 5	14
Supplementary Figure 6	15
Supplementary Figure 7	16
Supplementary Figure 8	17
Supplementary Figure 9	18
Supplementary Tables	19
Supplementary Table 1	19
Supplementary Table 2	20
Supplementary Table 3	21
Supplementary Table 4	22
Supplementary Table 5	23
Supplementary Table 6	24
Supplementary Table 7	25
Supplementary Table 8	26
Supplementary Table 9	27
Supplementary Table 10	28
References	29

Abbreviations

- **cMET**: hematoxylin/tyrosine-protein kinase met staining;
- **CASP8**: caspase 8 protein;
- **CIC**: cell-in-cell events;
- **CI(s)**: confidence interval(s);
- **CRC**: colorectal cancer;
- **DFS**: disease-free survival;
- **DR4**: death receptor 4;
- **DR5**: death receptor 5;
- **DSS**: disease-specific survival;
- **FLIP**: FLICE (FADD-like IL-1B-converting enzyme)-inhibitory protein;
- **HE**: hematoxylin/eosin staining;
- **HR**: hazard ratio;
- **IHC**: immunohistochemistry;
- **NI240**: Northern Ireland phase III clinical trial;
- **TMA**: tissue microarray;
- **TRAIL**: TNF-related apoptosis-inducing ligand.

Software packages

Complete datasets and analysis code are available via a [public BitBucket repository](#) and archived with Zenodo at [10.5281/zenodo.3841833](#). Analysis was performed in python (Van Rossum and Drake 2009), matlab (MATLAB 2014) and R (R Core Team 2020). The full list of packages and their versions are listed in the [repository binder folder](#). Key libraries, corresponding programming language and usage in this study are listed in the table below.

Language	Description	Package
Python	Data ingestion, cleaning and wrangling	<i>pandas</i> (McKinney and others 2010), <i>numpy</i> (Oliphant 2006)
Python	Data visualization	<i>matplotlib</i> (Hunter 2007), <i>seaborn</i> (Waskom et al. 2018), <i>upsetplot</i> (Alexander Lex 2014), <i>pydot</i> (wrapper for <i>graphviz</i> (Ellson et al. 2001)), <i>svgutils</i>
Python	Statistical analysis	<i>scipy</i> (Virtanen et al. 2020), <i>statsmodels</i> (Seabold and Perktold 2010), <i>tableone</i> (Pollard et al. 2018), <i>lifelines</i> (Davidson-Pilon 2019)
R	Statistical analysis	<i>glmmTMB</i> (Brooks et al. 2017), <i>car</i> (Fox and Weisberg 2019)
Matlab	Data visualization	<i>HCP</i> (<i>HeatmapCovariatePlot</i>) (Salvucci and Prehn 2019)

Figure panels for Figure 6 in the main manuscript

Figure 6 panel B

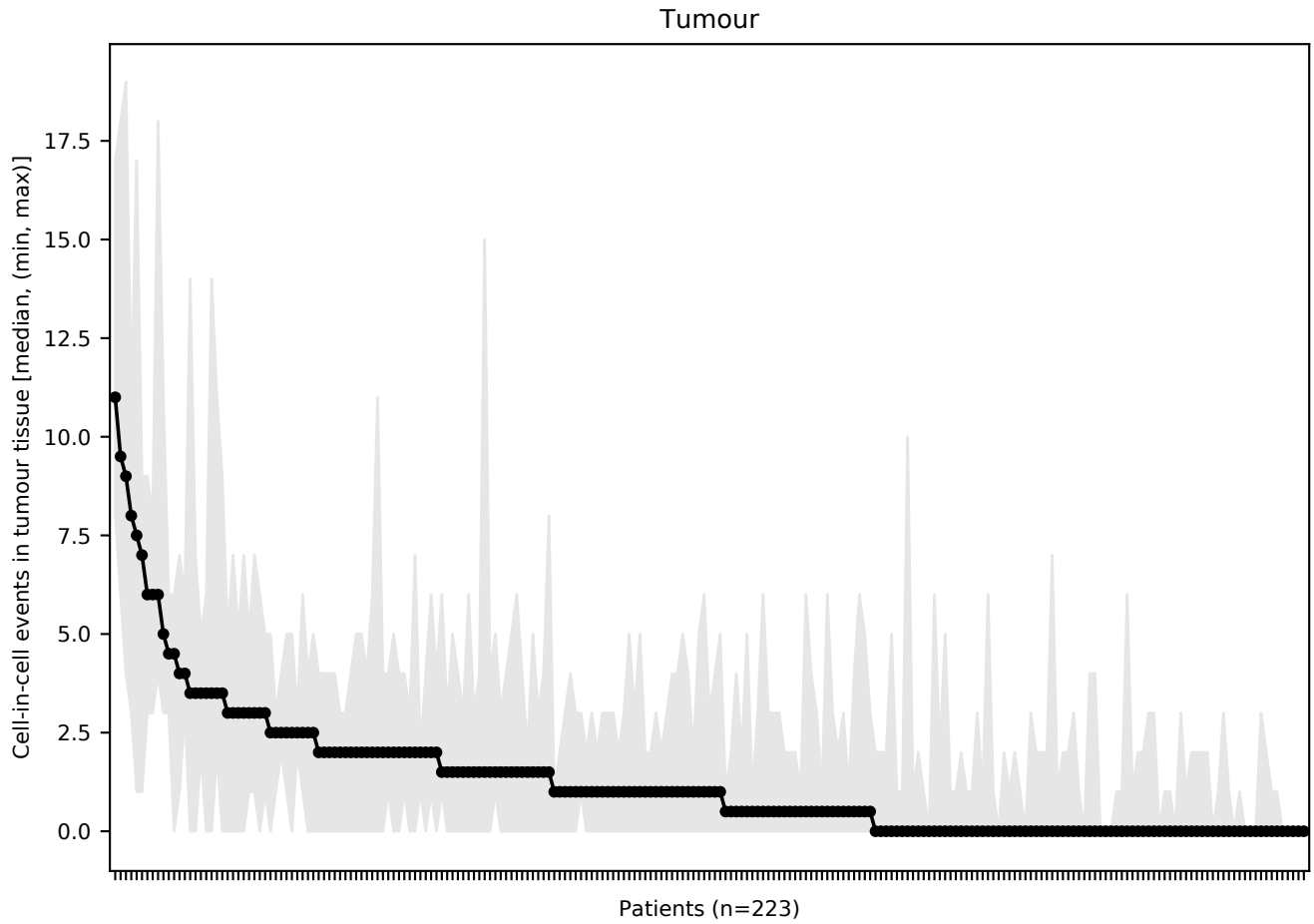


Fig. 6B. Inter- and intra-patient heterogeneity in cell-in-cell (CIC) events detected in tumor tissue and computed for each patient of the NI240 cohort. Patients (x-axis) are sorted in decreasing order of median CIC events (y-axis) detected in individual TMA cores prepared from tumour tissue and stained with either HE or cMET. Marker and shaded area indicate the median and the minimum/maximum CIC across the cores for each patient, respectively.

Figure 6 panel C

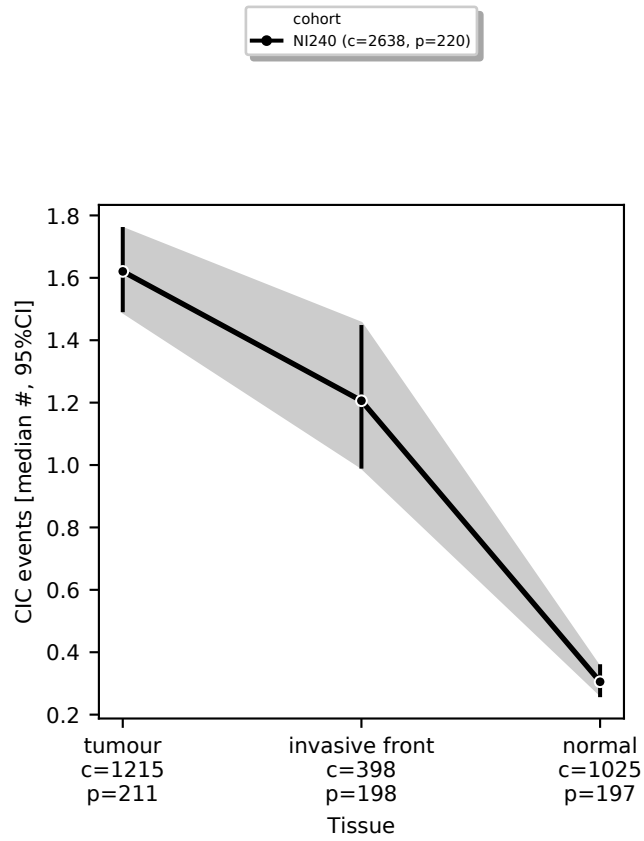


Fig. 6C. CIC events (median and 95% CI) detected in TMA sections prepared from tumour centre, invasive front and matched normal tissue. The letters “c” and “p” are abbreviations for “cores” and “patients”, respectively. Corresponding statistical analysis is reported in **Sup. Table 6**.

Figure 6 panel D

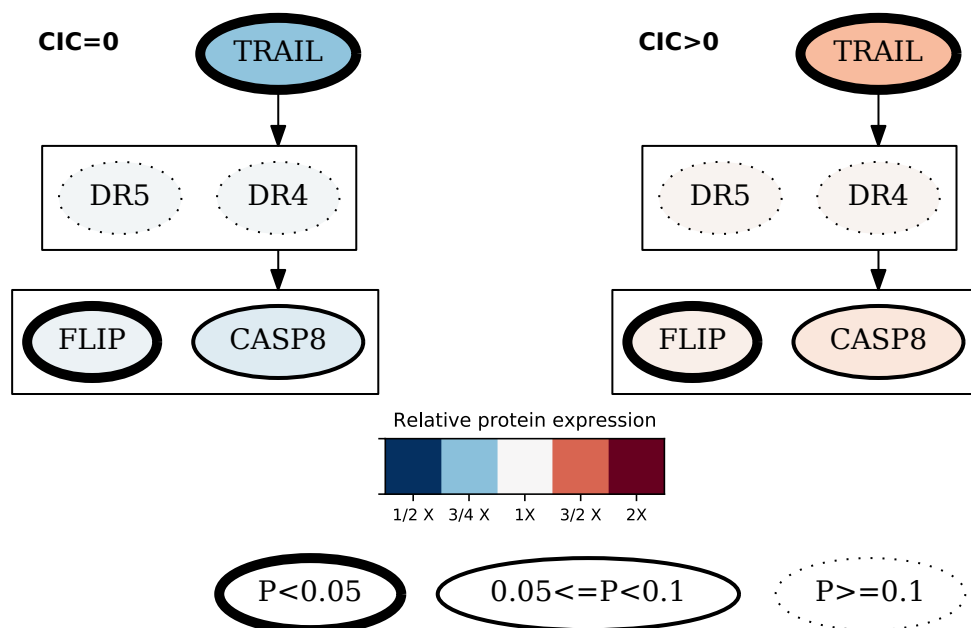


Fig. 6D. Association between expression of proteins involved in TRAIL signalling (TRAIL, DR4, DR5, CASP8 and FLIP) and CIC events. Relative protein expression between patients classified as CIC negative (CIC=0) or CIC-positive (CIC>0) based on the median CIC events observed across TMA sections prepared from tumour tissue is indicated in color. Red and blue shades indicate increased expression in CIC-positive or CIC-negative patients, respectively. Statistical significant differences in protein expression between CIC-negative and CIC-positive patients are encoded by the node edge style where solid tick lines and dotted thin lines indicate significant and non-significant differences, respectively. Visualization was generated with the python package *pydot*, built on *graphviz* (Ellson et al. 2001)). Complete statistical results are reported in **Sup. Table 8**.

Figure 6 panel F

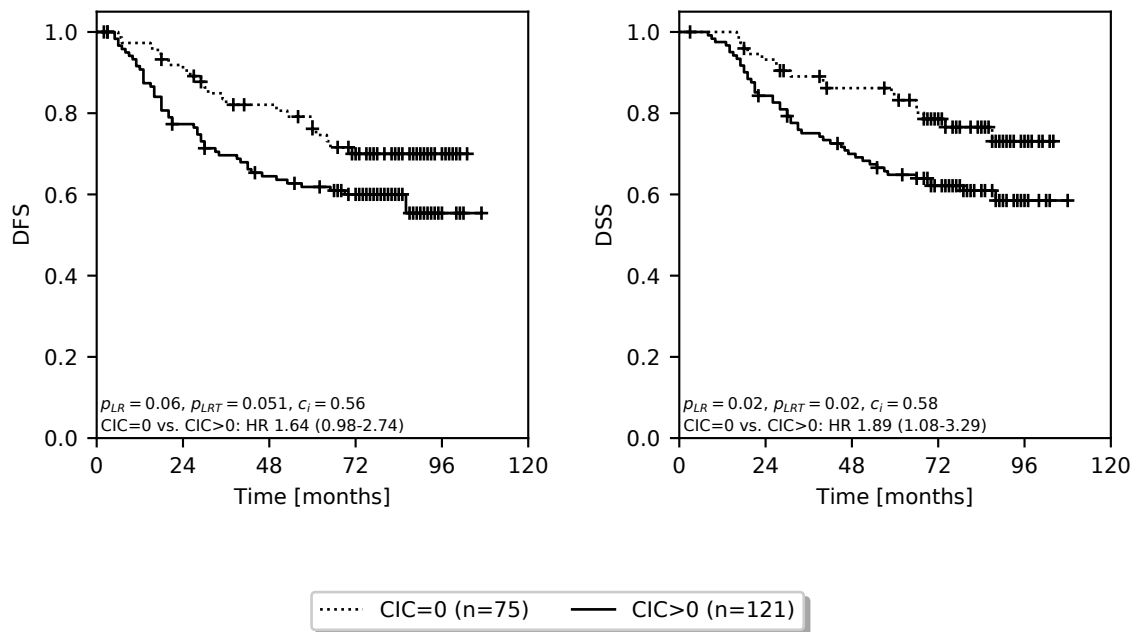


Fig. 6F. Kaplan-Meier estimates of DFS and DSS comparing stage II and III patients of the NI240 cohort grouped by the absence or presence of CIC events detected in the invasive front tissue. Patients were classified as CIC-negative (CIC=0) or CIC-positive (CIC>0) if the median number of CIC events detected across multiple biological replicas (TMA sections) prepared from the invasive front tissue was equal to or greater than zero, respectively. Kaplan-Meier estimators, logrank p-values and univariate Cox regression models were computed with the python package *lifelines*.

Figure 6 panel G

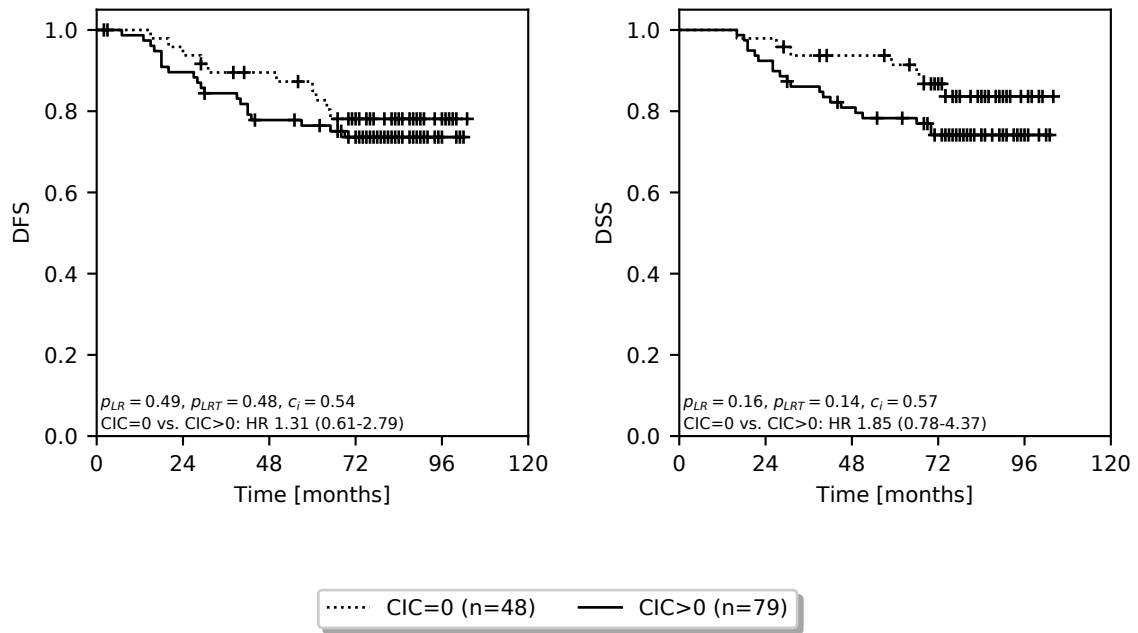


Fig. 6G. Kaplan-Meier estimates of DFS and DSS comparing stage II patients from the NI240 cohort grouped by the absence or presence of CIC events detected in the invasive front tissue. Patients were classified as CIC-negative (CIC=0) or CIC-positive (CIC>0) if the median number of CIC events detected across multiple biological replicas (TMA sections) prepared from the invasive front tissue was equal to or greater than zero, respectively. Kaplan-Meier estimators, logrank p-values and univariate Cox regression models were computed with the python package *lifelines*.

Figure 6 panel H

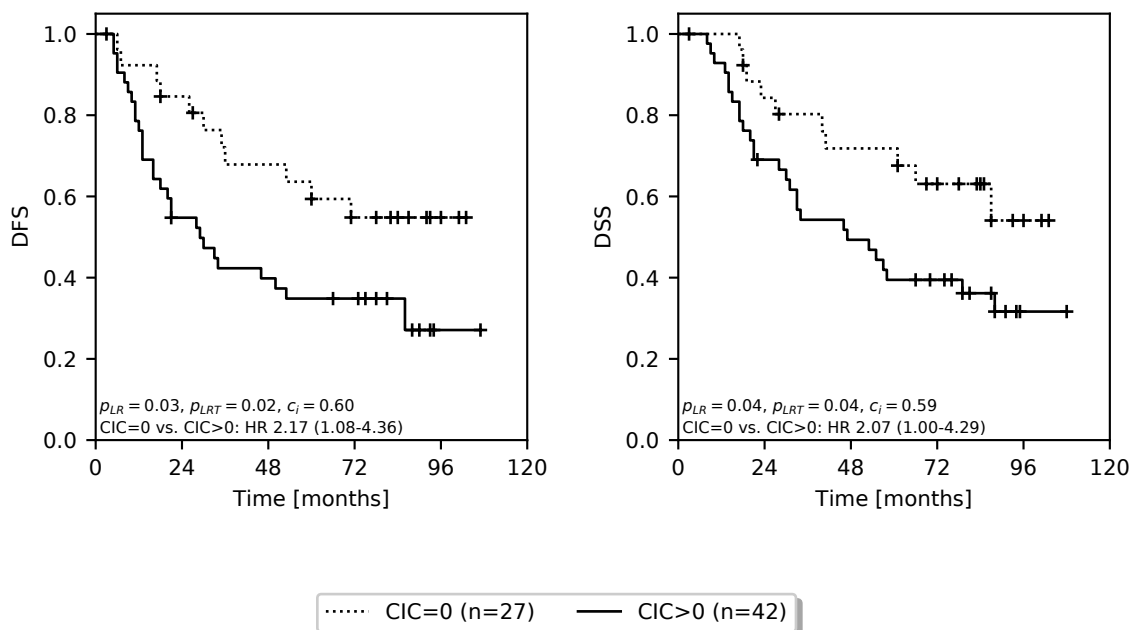
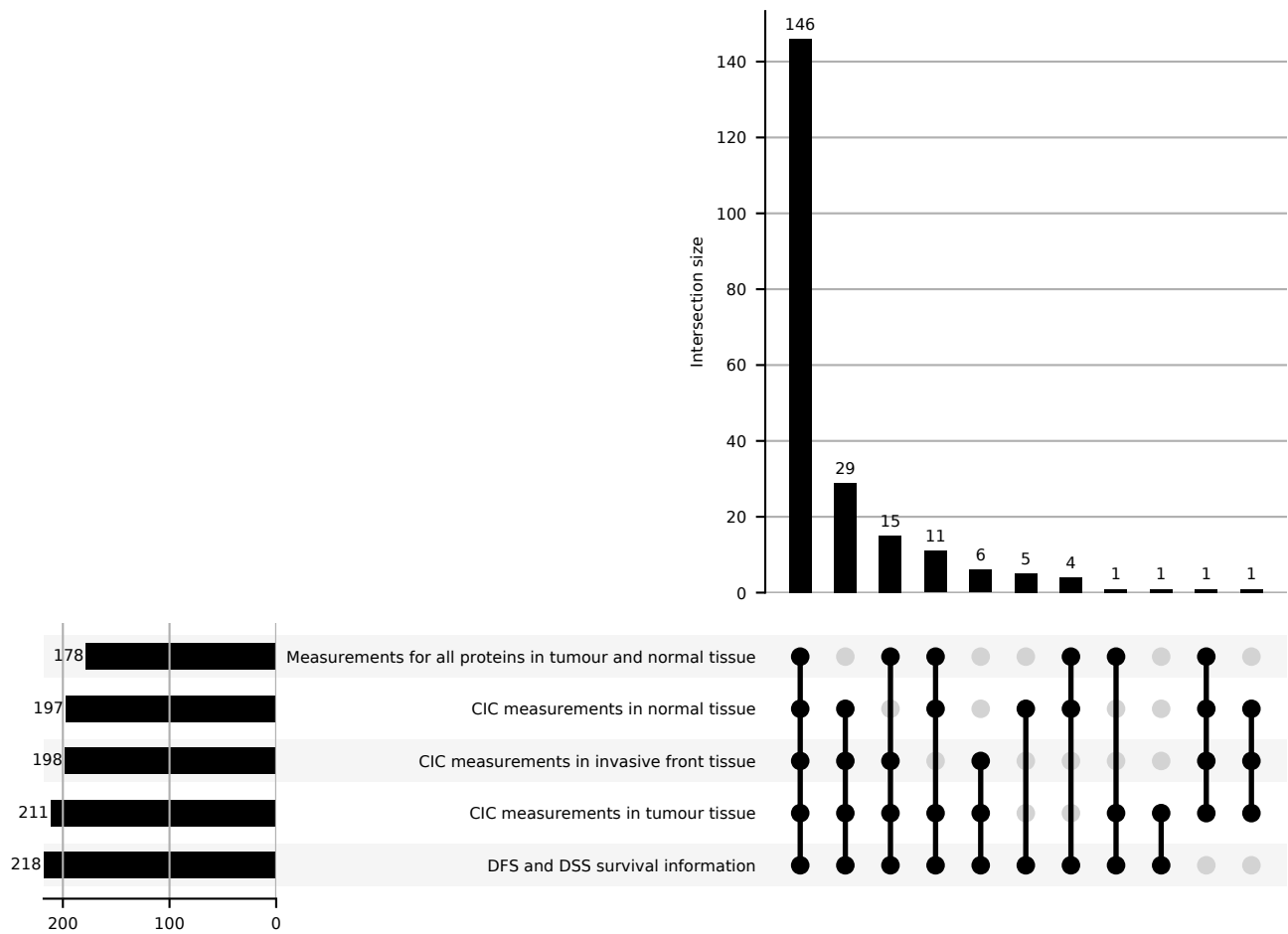


Fig. 6H. Kaplan-Meier estimates of DFS and DSS comparing stage III patients from the NI240 cohort grouped by the absence or presence of CIC events detected in the invasive front tissue. Patients were classified as CIC-negative (CIC=0) or CIC-positive (CIC>0) if the median number of CIC events detected across multiple biological replicas (TMA sections) prepared from the invasive front tissue was equal to or greater than zero, respectively. Kaplan-Meier estimators, logrank p-values and univariate Cox regression models were computed with the python package *lifelines*.

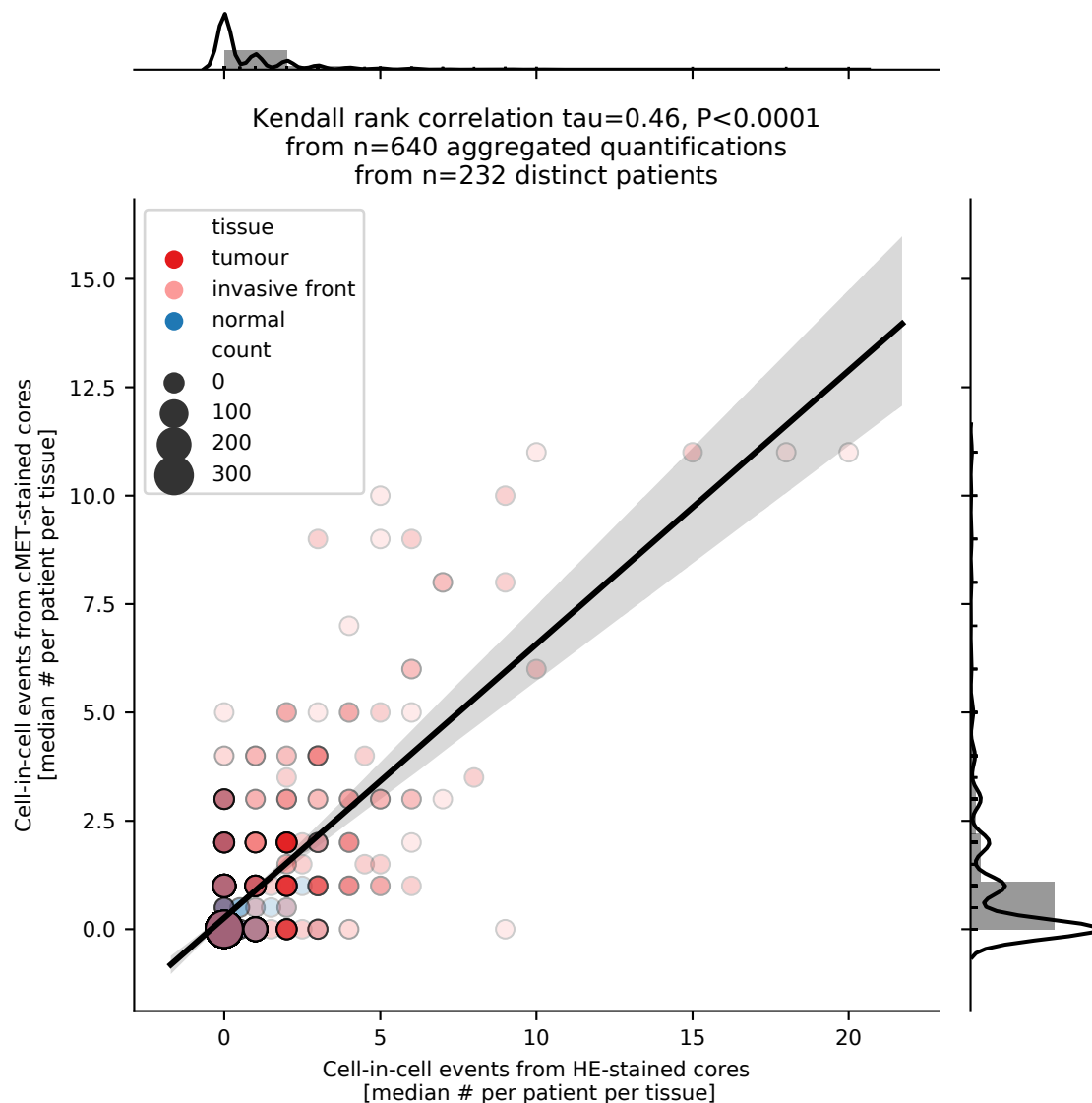
Supplementary Figures

Supplementary Figure 1



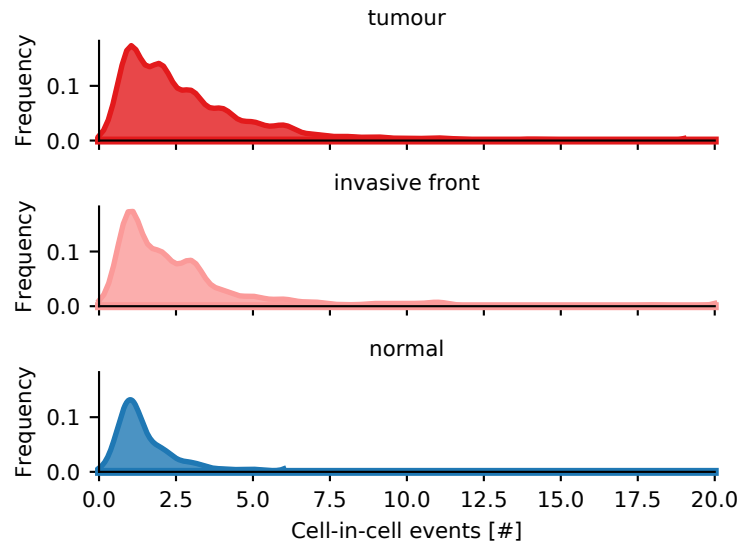
Sup. Fig. 1. Data availability per-patient. Figure panel indicating the total number of patients available for analysis of the association between the number of CIC events detected by tissue type (tumour, invasive front and normal), clinical outcome (DFS and DSS) and IHC measurements of TRAIL signalling proteins in tumour and normal tissue. Visualization was created with the python package *upsetplot*.

Supplementary Figure 2



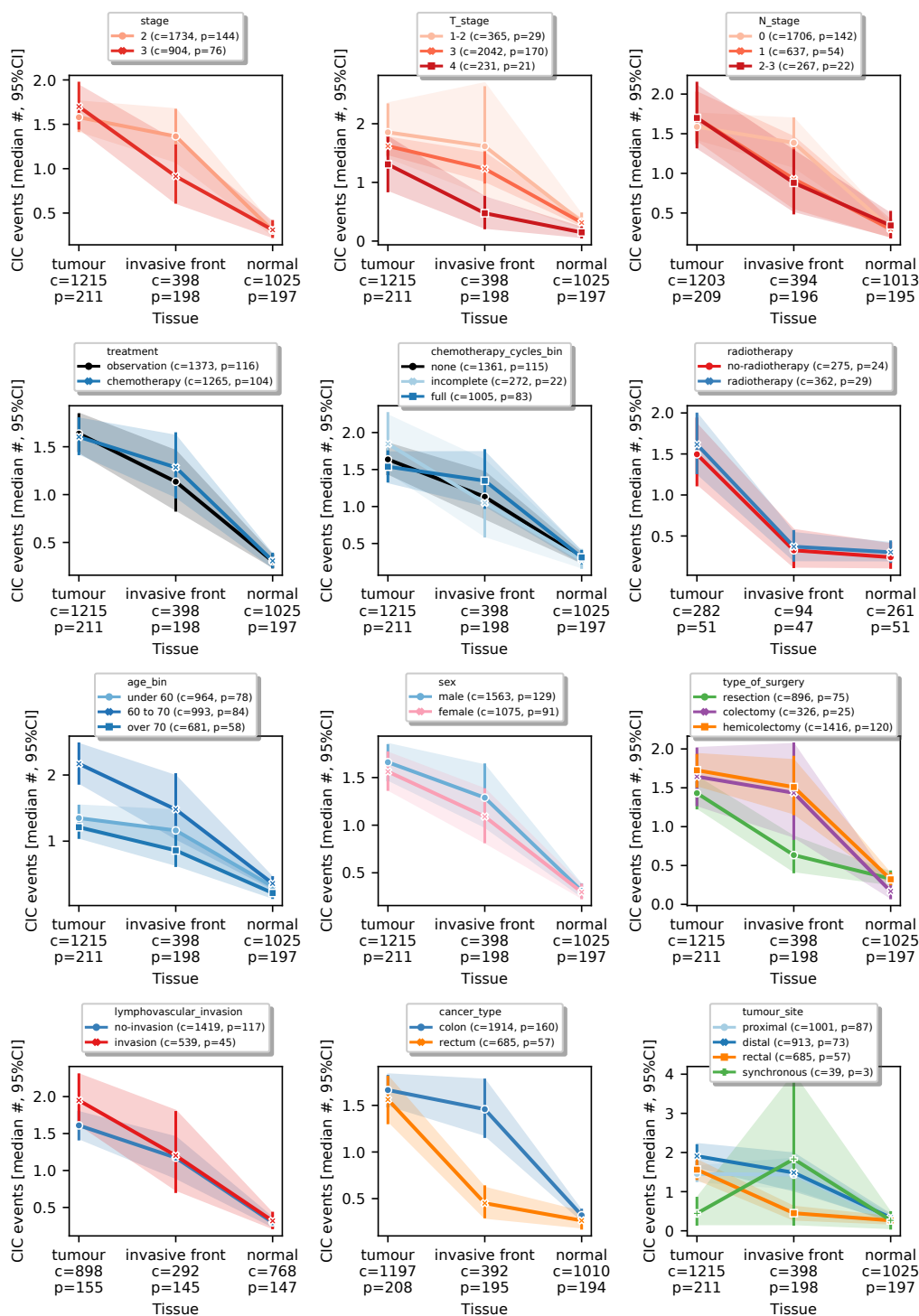
Sup. Fig. 2. Comparison between CIC events (median aggregated by patient, tissue and staining marker) observed in TMA sections stained for HE and cMET. Marker color indicates tissue type. Marker size and transparency encode the number of cores. Solid black line and gray shaded area indicate the regression line and CI, respectively. Agreement between CIC estimates from HE- and cMET-stained TMA cores was computed using the Kendall tau correlation (python package *scipy*).

Supplementary Figure 3



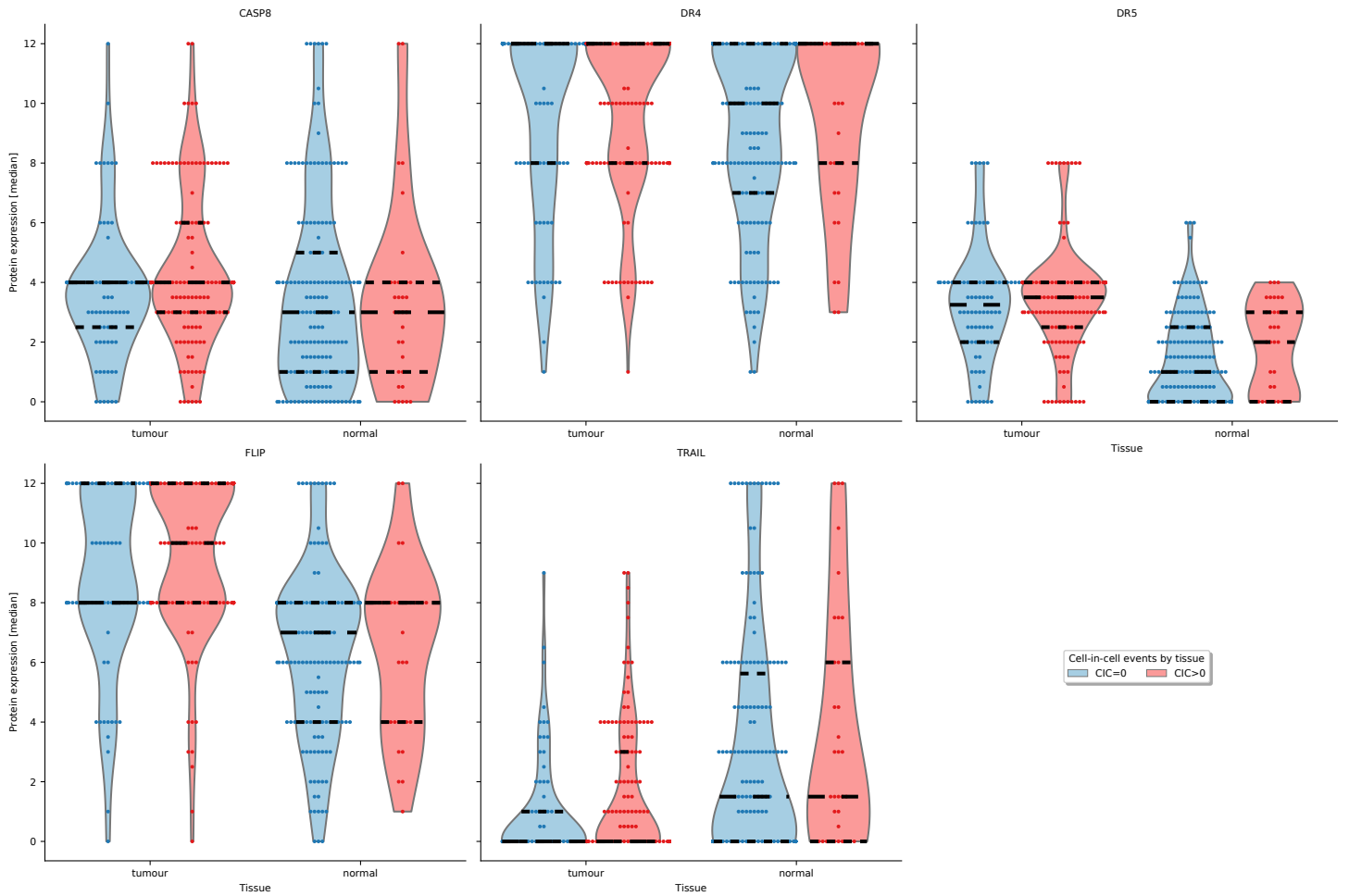
Sup. Fig. 3. Distribution of CIC events detected across all TMA sections examined (Sup. Tables 3-4) grouped by tissue type.

Supplementary Figure 4



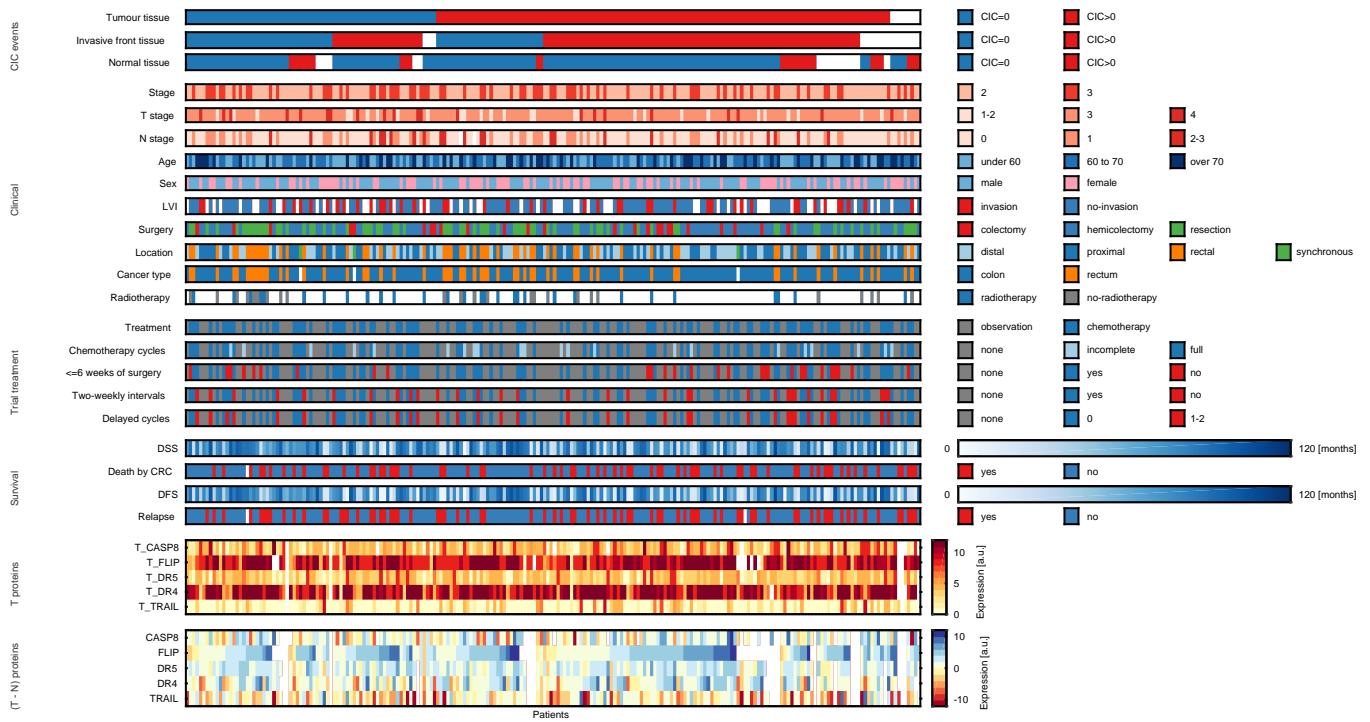
Sup. Fig. 4. CIC events (median and 95% CI) detected in TMA sections prepared from tumour centre, invasive front and matched normal tissue broken down by clinic-pathological characteristics. The letters “c” and “p” are abbreviations for “cores” and “patients”, respectively. Corresponding statistical analysis is reported in **Sup. Table 7**.

Supplementary Figure 5



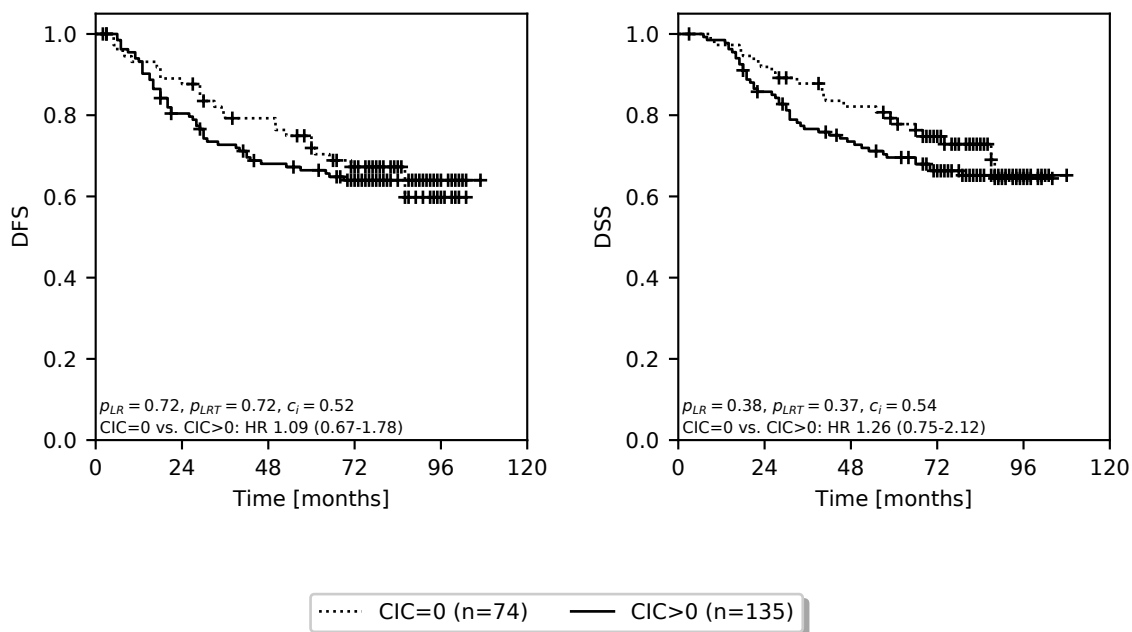
Sup. Fig. 5. Association between expression of key proteins involved in TRAIL signalling and CIC events. Protein expression was determined by IHC in TMA sections prepared from tumour and normal tissue and expressed as the product of the staining scores for intensity (0-3 integer scale) and coverage (0-4 integer scale). Protein expression across multiple biological replicas (cores) per patient per tissue type was aggregated by median and plotted grouped by absence (CIC=0) or presence (CIC>0) of CIC events in the corresponding tissue. Protein expression by tissue type and color-coded by CIC events group is shown as violin plot overlaid with individual measurements shown as swarmplot. Distribution quartiles are highlighted by tick dotted black lines. Corresponding statistical analysis (restricted to tumour tissue) is reported in **Sup. Table 8**.

Supplementary Figure 6



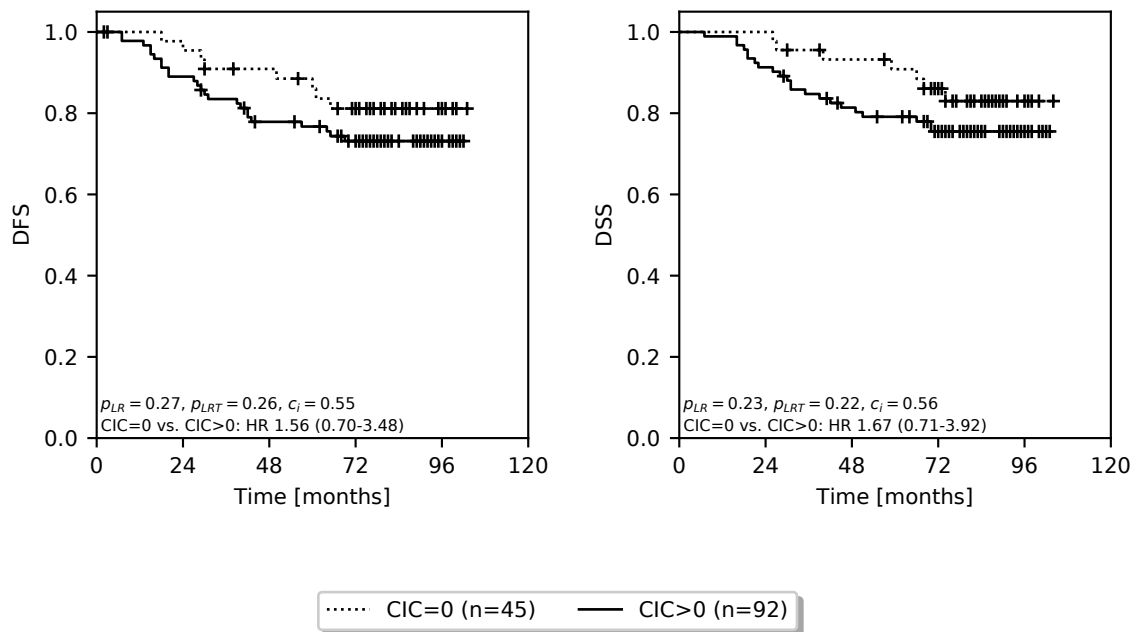
Sup. Fig. 6. Overview of clinical, demographic, pathological and molecular information for the CRC patients of the NI240 phase III clinical trial. Each column represents a patient and each row color-codes a feature. Missing data are shown in white. CIC-derived features include estimates of absence (CIC=0) or presence (CIC>0) of CIC events from TMA sections prepared from tumour, invasive front and normal tissue. Visualization was generated with the MATLAB package *HCP*.

Supplementary Figure 7



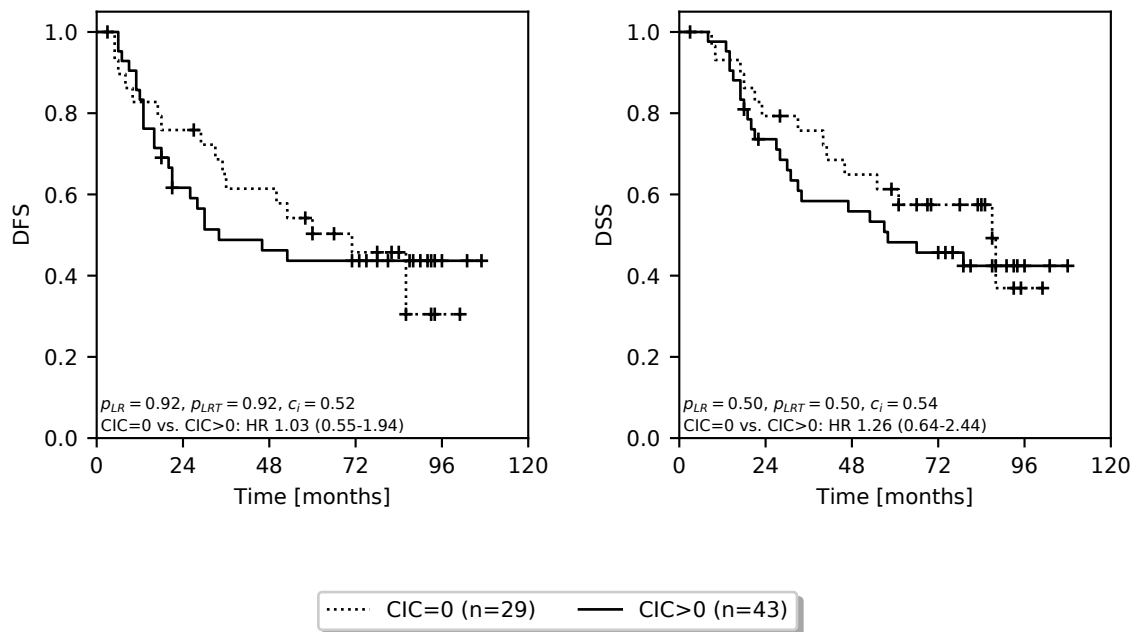
Sup. Fig. 7. Kaplan-Meier estimates of DFS and DSS comparing stage II and III patients of the NI240 cohort grouped by the absence or presence of CIC events detected in tumour tissue. Patients were classified as CIC-negative (CIC=0) or CIC-positive (CIC>0) if the median number of CIC events detected across multiple biological replicas (TMA sections) prepared from tumour tissue was equal to or greater than zero, respectively. Kaplan-Meier estimators, logrank p-values and univariate Cox regression models were computed with the python package *lifelines*.

Supplementary Figure 8



Sup. Fig. 8. Kaplan-Meier estimates of DFS and DSS comparing stage II patients of the NI240 cohort grouped by the absence or presence of CIC events detected in tumour tissue. Patients were classified as CIC-negative (CIC=0) or CIC-positive (CIC>0) if the median number of CIC events detected across multiple biological replicas (TMA sections) prepared from tumour tissue was equal to or greater than zero, respectively. Kaplan-Meier estimators, logrank p-values and univariate Cox regression models were computed with the python package *lifelines*.

Supplementary Figure 9



Sup. Fig. 9. Kaplan-Meier estimates of DFS and DSS comparing stage III patients of the NI240 cohort grouped by the absence or presence of CIC events detected in tumour tissue. Patients were classified as CIC-negative (CIC=0) or CIC-positive (CIC>0) if the median number of CIC events detected across multiple biological replicas (TMA sections) prepared from tumour tissue was equal to or greater than zero, respectively. Kaplan-Meier estimators, logrank p-values and univariate Cox regression models were computed with the python package *lifelines*.

Supplementary Tables

Supplementary Table 1

Sup. Table 1: Clinical, demographic and pathological characteristics of the patients of the NI240 phase III clinical trial. Summary statistics table was created with the python package *tableone*.

Variable	Level	Missing [n]	Chemotherapy	Observation	P-value	Test
n			117	122		
radiotherapy	no-radiotherapy	179	10 (36)	17 (53)	0.275	Chi-squared
	radiotherapy		18 (64)	15 (47)		
cancer type	colon	4	83 (73)	88 (72)	0.936	Chi-squared
	rectum		30 (27)	34 (28)		
type of surgery	colectomy	0	9 (8)	17 (14)	0.181	Chi-squared
	hemicolectomy		69 (59)	60 (49)		
	resection		39 (33)	45 (37)		
stage	2	0	77 (66)	79 (65)	0.971	Chi-squared
	3		40 (34)	43 (35)		
T stage	1-2	0	15 (13)	18 (15)	0.706	Chi-squared
	3		89 (76)	94 (77)		
	4		13 (11)	10 (8)		
N stage	0	2	75 (65)	79 (65)	0.975	Chi-squared
	1		28 (24)	31 (25)		
	2-3		12 (10)	12 (10)		
grade	1	10	9 (8)	10 (9)	0.889	Chi-squared
	2		88 (78)	92 (79)		
	3		16 (14)	14 (12)		
age		0	65 [58,70]	65 [56,72]	0.958	Kruskal-Wallis
sex	female	0	50 (43)	46 (38)	0.509	Chi-squared
	male		67 (57)	76 (62)		
lymphovascular invasion	invasion	63	25 (29)	23 (26)	0.794	Chi-squared
	no-invasion		62 (71)	66 (74)		

Supplementary Table 2

Sup. Table 2: Clinical follow-up computed with the python package *lifelines* for the patients of the NI240 phase III clinical trial.

Endpoint	# patients	Median [months]	2.5% CI [months]	97.5% CI [months]
DFS	237	82	80	84
DSS	238	83	80	85

Supplementary Table 3

Sup. Table 3: Breakdown of the number of TMA cores analyzed for CIC events per patient per tissue from n=232 distinct patients of the NI240 phase III clinical trial.

Tissue	Total # patients	Total # cores	Median # cores per-patient	Min # cores per-patient
tumour	223	1284	6	2
invasive front	209	420	2	2
normal	209	1087	6	2

Supplementary Table 4

Sup. Table 4: Breakdown of the number of TMA cores analyzed for CIC events per marker, tissue and slide from n=232 distinct patients of the NI240 phase III clinical trial.

Marker	Tissue	Slide	# patients
HE	tumour	A	219
		B	221
		C	208
HE	invasive front	D	210
HE	normal	E	187
		F	190
		G	175
cMET	tumour	A	210
		B	216
		C	210
cMET	invasive front	D	210
cMET	normal	E	174
		F	186
		G	175

Supplementary Table 5

Sup. Table 5: Breakdown of the number of TMA cores analyzed for CIC events per patient per tissue for protein expression by IHC for the NI240 phase III clinical trial.

Tissue	Protein	Total # patients	Total # cores	Median # cores per-patient	Min # cores per-patient
tumour	CASP8	223	4150	4	1
	DR4	227	4150	4	1
	DR5	229	4150	4	1
	FLIP	221	4150	4	1
	TRAIL	230	4150	4	1
normal	CASP8	210	3451	3	1
	DR4	213	3451	4	1
	DR5	217	3451	4	1
	FLIP	206	3451	4	1
	TRAIL	218	3451	4	1

Supplementary Table 6

Sup. Table 6: Dependency of the number of observed CIC events detected in TMA sections by tissue type. For statistical analysis, a zero-inflated Poisson regression model, including a random effect for each patient, was fit (R package [glmmTMB](#) and [car](#)). Number of cores included, effect sizes (estimates), 95% CIs and p-values computed by likelihood ratio tests were reported.

Term	Ref-level	Level	Estimate	2.5 %	97.5 %	P	# cores
tissue						<0.0001	606
	tumour	invasive front	-0.06	-0.23	0.12		606
		normal	-2.36	-2.78	-1.94		606

Supplementary Table 7

Sup. Table 7: Association between number of observed CIC events detected in TMA sections and clinical, demographic or pathological covariates by tissue type. Variables were selected *a priori*. For statistical analysis, a zero-inflated Poisson regression model, including a random effect for each patient and covariate-fixed effects, was fitted (R package *glmmTMB* and *car*). Number of cores included, effect sizes (estimates) for the variable of interest, 95% CIs and p-values computed by likelihood ratio tests were reported.

Term	Ref-level	Level	Estimate	2.5 %	97.5 %	P	# cores
stage						0.39	606
	2	3	-0.14	-0.45	0.18		606
T stage						0.07	606
	1-2	3	-0.01	-0.45	0.43		606
		4	-0.67	-1.36	0.01		606
N stage						0.58	600
	0	1	-0.19	-0.56	0.17		600
		2-3	-0.05	-0.55	0.45		600
age						0.13	606
	under 60	60 to 70	0.22	-0.11	0.56		606
		over 70	-0.15	-0.54	0.24		606
sex						0.66	606
	male	female	-0.07	-0.37	0.24		606
type of surgery						0.06	606
	resection	colectomy	0.32	-0.18	0.82		606
		hemicolectomy	0.40	0.07	0.73		606
cancer type						0.009	597
	colon	rectum	-0.47	-0.82	-0.12		597
tumour site						0.054	606
	proximal	distal	0.15	-0.18	0.49		606
		rectal	-0.40	-0.78	-0.01		606
		synchronous	-0.17	-1.45	1.10		606
lymphovascular invasion						0.56	447
	no-invasion	invasion	0.11	-0.27	0.49		447
treatment						0.49	606
	observation	chemotherapy	0.11	-0.19	0.40		606
radiotherapy						0.53	149
	no-radiotherapy	radiotherapy	0.21	-0.45	0.87		149
chemotherapy cycles						0.71	606
	none	full	0.09	-0.23	0.41		606
		incomplete	0.19	-0.32	0.69		606

Supplementary Table 8

Sup. Table 8: Association between expression of proteins involved in TRAIL signalling and CIC events observed in tumour tissue of CRC patients of the NI240 phase III clinical trial. Protein expression determined by IHC across biological replicas of tumour sections (**Sup. Table 5**) and per patient were aggregated by the median. CIC events observed across multiple biological TMA cores prepared from tumour tissue were aggregated by median and binarised into absence (CIC=0) or presence (CIC>0). Statistical analysis was performed with the python package [statsmodels](#) by univariate unadjusted linear models and effect sizes, 95% CIs, p-values and number of patients included in each analysis were reported.

Protein	Unadjusted statistics
CASP8	CIC>0 (ref. CIC=0): 0.66, 95% CI -0.02-1.35, P=0.06, n=216
DR4	CIC>0 (ref. CIC=0): 0.37, 95% CI -0.44-1.18, P=0.37, n=220
DR5	CIC>0 (ref. CIC=0): 0.12, 95% CI -0.38-0.62, P=0.65, n=222
FLIP	CIC>0 (ref. CIC=0): 0.78, 95% CI 0.00-1.55, P=0.049, n=213
TRAIL	CIC>0 (ref. CIC=0): 0.59, 95% CI 0.02-1.15, P=0.04, n=222

Supplementary Table 10

Sup. Table 10: Univariate and multivariate Cox regression models for stage III patients of the NI240 phase III clinical trial. Univariate models were fitted for baseline clinical, demographic and pathological characteristics and features derived from CIC events observed in TMA sections prepared from tumour, invasive front and normal tissue. For CIC events-based features, patients were grouped based on the absence (CIC=0) or presence (CIC>0) of CIC events computed as median across multiple cores for the corresponding tissue. The multivariate model included CIC events feature derived from the invasive front and was adjusted by baseline patient characteristics selected *a priori*. HRs, 95% CIs, p-values computed by loglikelihood ratio tests, *c*-indices and number of included patients were reported. Cox regression models were fitted using the python package *lifelines*.

Model type	Term	Ref level	Level	DFS						DSS									
				HR (95% CI)	HR	2.5% CI	97.5% CI	Per-term P-value	Per-model P-value	C-index	N	HR (95% CI)	HR	2.5% CI	97.5% CI	Per-term P-value	Per-model P-value	C-index	N
univariate	treatment	observation	chemotherapy	●	0.52	0.28	0.96	0.03	0.03	0.60	75	●	0.60	0.31	1.13	0.11	0.11	0.57	75
			age	●	0.99	0.96	1.03	0.77	0.77	0.49	75	●	0.99	0.95	1.02	0.46	0.46	0.53	75
	sex	male	female	●	1.08	0.58	2.01	0.80	0.80	0.51	75	●	1.35	0.71	2.54	0.36	0.36	0.54	75
			cancer type	colon	rectum	●	1.10	0.57	2.13	0.77	0.77	0.51	75	●	1.01	0.51	1.99	0.98	0.98
	type of surgery	resection	colectomy	●	0.79	0.23	2.71	0.86	0.86	0.51	75	●	1.03	0.30	3.56	1.00	1.00	0.53	75
			hemicolectomy	●	0.85	0.45	1.60	0.92	0.92	0.52	72	●	1.02	0.52	1.97	0.50	0.50	0.54	72
	CIC in tumour tissue	T-CIC=0	T-CIC>0	●	1.03	0.55	1.94	0.02	0.02	0.60	69	●	1.26	0.64	2.44	0.04	0.04	0.59	69
	CIC in invasive front tissue	S-CIC=0	S-CIC>0	●	2.17	1.08	4.36	0.50	0.50	0.52	65	●	2.07	1.00	4.29	0.75	0.75	0.51	65
	CIC in normal tissue	N-CIC=0	N-CIC>0	●	0.68	0.21	2.22	0.01	0.01	0.69	69	●	0.83	0.25	2.72	0.06	0.06	0.67	69
	multivariate	treatment	observation	chemotherapy	●	0.36	0.18	0.71	0.003				●	0.43	0.21	0.87	0.02		
age				●	1.01	0.97	1.04	0.76				●	0.99	0.95	1.02	0.49			
sex		male	female	●	1.13	0.59	2.18	0.72				●	1.47	0.73	2.95	0.28			
			cancer type	colon	rectum	●	1.45	0.70	2.97	0.32			●	1.09	0.52	2.25	0.83		
CIC in invasive front tissue	S-CIC=0	S-CIC>0	●	2.67	1.31	5.43	0.004				●	2.33	1.12	4.87	0.02				

References

- Alexander Lex, Hendrik Strobelt, Nils Gehlenborg. 2014. “UpSet: Visualization of Intersecting Sets.” *IEEE Transactions on Visualization and Computer Graphics* 20 (12): 1983–92. <https://doi.org/10.1109/TVCG.2014.2346248>.
- Brooks, Mollie E., Kasper Kristensen, Koen J. van Benthem, Arni Magnusson, Casper W. Berg, Anders Nielsen, Hans J. Skaug, Martin Maechler, and Benjamin M. Bolker. 2017. “glmmTMB Balances Speed and Flexibility Among Packages for Zero-Inflated Generalized Linear Mixed Modeling.” *The R Journal* 9 (2): 378–400. <https://journal.r-project.org/archive/2017/RJ-2017-066/index.html>.
- Davidson-Pilon, Cameron. 2019. “Lifelines: Survival Analysis in Python.” *Journal of Open Source Software* 4 (40): 1317. <https://doi.org/10.21105/joss.01317>.
- Ellson, John, Emden Gansner, Lefteris Koutsofios, Stephen North, Gordon Woodhull, Short Description, and Lucent Technologies. 2001. “Graphviz — Open Source Graph Drawing Tools.” In *Lecture Notes in Computer Science*, 483–84. Springer-Verlag.
- Fox, John, and Sanford Weisberg. 2019. *An R Companion to Applied Regression*. Third. Thousand Oaks CA: Sage. <https://socialsciences.mcmaster.ca/jfox/Books/Companion/>.
- Hunter, John D. 2007. “Matplotlib: A 2D Graphics Environment.” *Computing in Science & Engineering* 9 (3): 90–95.
- MATLAB. 2014. *Version 8.4.0 (R2014b)*. Natick, Massachusetts: The MathWorks Inc.
- McKinney, Wes, and others. 2010. “Data Structures for Statistical Computing in Python.” In *Proceedings of the 9th Python in Science Conference*, 445:51–56. Austin, TX.
- Oliphant, Travis E. 2006. *A Guide to Numpy*. Vol. 1. Trelgol Publishing USA.
- Pollard, Tom J, Alistair E W Johnson, Jesse D Raffa, and Roger G Mark. 2018. “tableone: An open source Python package for producing summary statistics for research papers.” *JAMIA Open* 1 (1): 26–31. <https://doi.org/10.1093/jamiaopen/ooy012>.
- R Core Team. 2020. *R: A Language and Environment for Statistical Computing*. Vienna, Austria: R Foundation for Statistical Computing. <https://www.R-project.org/>.
- Salvucci, Manuela, and Jochen H. m. Prehn. 2019. “HCP: A Matlab Package to Create Beautiful Heatmaps with Richly Annotated Covariates.” *Journal of Open Source Software* 4 (38): 1291. <https://doi.org/10.21105/joss.01291>.
- Seabold, Skipper, and Josef Perktold. 2010. “Statsmodels: Econometric and Statistical Modeling with Python.” In *9th Python in Science Conference*.
- Van Rossum, Guido, and Fred L. Drake. 2009. *Python 3 Reference Manual*. Scotts Valley, CA: CreateSpace.
- Virtanen, Pauli, Ralf Gommers, Travis E. Oliphant, Matt Haberland, Tyler Reddy, David Cournapeau, Evgeni Burovski, et al. 2020. “SciPy 1.0: Fundamental Algorithms for Scientific Computing in Python.” *Nature Methods*. <https://doi.org/https://doi.org/10.1038/s41592-019-0686-2>.
- Waskom, Michael, Olga Botvinnik, Drew O’Kane, Paul Hobson, Saulius Lukauskas, David C Gemperline, Tom Augspurger, et al. 2018. *Mwaskom/Seaborn: V0.9.0 (July 2018)* (version v0.9.0). Zenodo. <https://doi.org/10.5281/zenodo.1313201>.